Roles of Germination-Specific Lytic Enzymes CwlJ and SleB in *Bacillus anthracis*[∇][†]

Jared D. Heffron, Benjamin Orsburn, and David L. Popham*

Department of Biological Sciences, Virginia Tech, Blacksburg, Virginia 24061

The structural characteristics of a spore enable it to withstand stresses that typically kill a vegetative cell. Spores remain dormant until small molecule signals induce them to germinate into vegetative bacilli. Germination requires degradation of the thick cortical peptidoglycan by germination-specific lytic enzymes (GSLEs). *Bacillus anthracis* has four putative GSLEs, based upon sequence similarities with enzymes in other species: SleB, CwlJ1, CwlJ2, and SleL. In this study, the roles of SleB, CwlJ1, and CwlJ2 were examined. The expression levels of all three genes peak 3.5 h into sporulation. Genetic analysis revealed that, similar to other known GSLEs, none of these gene products are individually required for growth, sporulation, or triggering of germination. However, later germination events are affected in spores lacking CwlJ1 or SleB. Compared to the wild type, germinating spores without CwlJ1 suffer a delay in optical density loss and cortex peptidoglycan release. The absence of SleB also causes a delay in cortex fragment release. A double mutant lacking both SleB and CwlJ1 is completely blocked in cortex hydrolysis and progresses through outgrowth to produce colonies at a frequency 1,000-fold lower than that of the wild-type strain. A null mutation eliminating CwlJ2 has no effect on germination. High-performance liquid chromatography and mass spectroscopy analysis revealed that SleB is required for lytic transglycosylase activity. CwlJ1 also clearly participates in cortex hydrolysis, but its specific mode of action remains unclear. Understanding the lytic germination activities that naturally diminish spore resistance can lead to methods for prematurely inducing them, thus simplifying the process of treating contaminated sites.

The spore of *Bacillus anthracis* is the infectious agent of the disease anthrax. Once entry to a suitable host has occurred, the endospore must undergo germination before it can produce any deadly toxins (12, 30). The bacterial endospore is a modified cell where the cytoplasm (spore core) is relatively dehydrated and surrounded by a thick peptidoglycan (PG) wall, called the cortex. As a result, the spore is metabolically dormant and strongly resistant to environmental insults (42). The cortex plays a major role in maintaining spore resistance by limiting the amount of water present in the core (42).

Although the spore is insensitive to environmental challenges, it remains responsive to particular chemical germinants. Contact with these germinants to a spore's germinant receptors can induce germination and outgrowth into a vegetative cell (11). There are three major events that occur once germination has been signaled. The first is that the spore core starts to rehydrate as water moves inward (36). The second event, likely coupled with the first, is transport of ions and dipicolinic acid (DPA) out of the core (9, 23, 30, 36). The third major step during germination includes the degradation of spore cortex PG by germination-specific lytic enzymes (GSLEs) and the release of muropeptides into the surrounding environment (30). At this point, the spore core is now free to expand fully and proceed toward a vegetative cell cycle (29).

PG consists of a repeating disaccharide of β-1,4-linked *N*-acetylglucosamine (NAG) and *N*-acetylmuramic acid (NAM). The NAM residue has a peptide side chain extending from the lactyl group, which is able to form a bond with a peptide chain on another PG strand, resulting in a cross-linked network surrounding the entire cell (40). This structure accurately describes the thin innermost layer of PG that encases an endospore. Termed the germ cell wall, this layer may serve as the foundation for newly synthesized PG after germination. The second layer of PG around endospores, referred to as the cortex, composes >80% of the total spore PG (26). It has a defining modification where as much as 50% of the NAM is converted to muramic-δ-lactam (26). During germination, the cortex, but not the germ cell wall, is broken down.

GSLEs have been shown to degrade only PG with muramic-δ-lactam, thus explaining cortex-exclusive breakdown (37, 41). In *Bacillus subtilis*, two GSLEs in particular appear crucial to germination: *cwlJ* and *sleB* (1, 16). CwlJ is expressed under the control of the mother cell sporulation factor σ^E, and evidence suggests that it ultimately localizes to the spore coat (3, 16). Proper localization, and hence function, is dependent on the product of *gerQ* (39). CwlJ is required for germination in response to Ca^2+-DPA; however, its specific enzymatic activity on PG remains a mystery (29, 36). CwlJ shows 30% sequence identity to the proposed catalytic domain of the other main GSLE of *B. subtilis*, SleB. SleB has an N-terminal putative cell wall-binding domain and is required for the appearance of lytic transglycosylase activity during germination of *B. subtilis* spores (1). Mature SleB and its homologs localize to the spore cortex and inner membrane in *Bacillus cereus* (33), *B.*

* Corresponding author. Mailing address: Department of Biological Sciences, Virginia Tech, Life Sciences I, MC0910, Washington St., Blacksburg, VA 24061. Phone: (540) 231-2529. Fax: (540) 231-4043. E-mail: dpopham@vt.edu.

TABLE 1. *B. anthracis* strains and plasmids

Strain or plasmid	Relevant genotype[a]	Construction[b]	Source or reference
Strains			
Sterne 34F2	pX01$^+$ pX02$^-$		P. Hanna
DPBa18	*cwlJ2*::pDPV331 (*cwlJ2'-lacZ* Kan^r *lacI* P$_{spac}$-*cwlJ2*)	pDPV331 → 34F2	This work
DPBa22	*cwlJ1*::pDPV330 (*cwlJ1'-lacZ* Kan^r *lacI* P$_{spac}$-*cwlJ1*)	pDPV330 → 34F2	This work
DPBa24	*sleB*::pDPV329 (*sleB'-lacZ* Kan^r *lacI* P$_{spac}$-*sleB*)	pDPV329 → 34F2	This work
DPBa38	Δ*sleB*	pDPV383 → 34F2	This work
DPBa57	Δ*sleB*; pDPV346 (*sleB*$^+$ Er^r)	pDPV346 → DPBa38	This work
DPBa59	Δ*sleB*; pBKJ236 (Er^r)	pBKJ236 → DPBa38	This work
DPBa61	Δ*cwlJ1*	pDPV347 → 34F2	This work
DPBa62	Δ*cwlJ1*; pBKJ236 (Er^r)	pBKJ236 → DPBa61	This work
DPBa63	Δ*cwlJ1*; pDPV345 (*cwlJ1*$^+$ Er^r)	pDPV345 → DPBa61	This work
Plasmids			
pDONRtet	Tet^r		11
pNFd13	Kan^r; pE194 *ori*(Ts); P$_{spac}$; *lacZ*		11
pBKJ223	Tet^r; P$_{amy}$-ISceI		17
pBKJ236	Er^r; *ori*(Ts)		17
pDPV329	P$_{spac}$-*sleB'-lacZ* Kan^r *lacI*	pNFd13::*sleB'*	This study
pDPV330	P$_{spac}$-*cwlJ1'-lacZ* Kan^r *lacI*	pNFd13::*cwlJ1'*	This study
pDPV331	P$_{spac}$-*cwlJ2'-lacZ* Kan^r *lacI*	pNFd13::*cwlJ2'*	This study
pDPV345	*cwlJ1*$^+$	pBKJ236::*cwlJ1*	This study
pDPV347	Δ*cwlJ1*	pBKJ236::Δ*cwlJ1*	This study
pDPV346	*sleB*$^+$	pBKJ236::*sleB*	This study
pDPV383	Δ*sleB*	pBKJ236::Δ*sleB*	This study

[a] Abbreviations for antibiotic resistance markers: Kan, kanamycin; Er, erythromycin; Tet, tetracycline.
[b] Strains were constructed by electroporation or conjugation. The designation preceding the arrow is the plasmid and the designation following the arrow is the recipient strain.

subtilis (8, 25), and *B. anthracis* (21). Expression of *sleB* is controlled by σ^G in the forespore (32). In *B. subtilis*, proper function of SleB is dependent on *ypeB*, which is located downstream of and included in a bicistronic operon with *sleB* (5, 8).

This study investigated three putative *B. anthracis* GSLEs, referred to as SleB, CwlJ1, and CwlJ2. Using null mutants, we show that SleB and CwlJ1 play significant roles in *B. anthracis* spore cortex hydrolysis. Both *sleB* and *cwlJ1* are expressed in a manner consistent with that observed in *B. subtilis*. We find that SleB is required for lytic transglycosylase activity. CwlJ2 is poorly expressed and plays no evident role in germination.

MATERIALS AND METHODS

Bacterial strains and antibiotics. All *B. anthracis* strains used in this study are derived from the Sterne strain 34F2 and are listed in Table 1. Electroporation of *B. anthracis* was performed as described previously (38). Transformants were selected on LB-1% glucose plates containing the appropriate antibiotics: 5 μg/ml erythromycin (Fisher), 50 μg/ml kanamycin sulfate (Jersey Lab Supply), or 10 μg/ml tetracycline (Jersey Lab Supply). Vegetative growth in brain heart infusion (BHI; Difco) medium with the corresponding antibiotic was examined for each strain, at 37°C for deletion mutants and 39°C for insertion mutants. Insertion mutant strains were sporulated in modified G (Mod G) medium without antibiotics (18) at 39°C with shaking for 3 days. Deletion mutants were similarly sporulated at 37°C, except for strains used for complementation experiments, which were cultivated at room temperature in Mod G containing the appropriate antibiotic. All spores were harvested by centrifugation, and vegetative cells were killed by incubation at 65°C for 25 min. Further spore purification was done with water washing and density centrifugation over 50% sodium diatrizoate (Sigma) as previously described (34).

Maintenance of pNFd13 containing the counterselectable marker *ccdB* was done with the One Shot *ccdB* Survival strain of *Escherichia coli*, available from Invitrogen. *E. coli* was grown in LB medium containing 10 μg/ml tetracycline hydrochloride (Jersey Lab Supply), 30 μg/ml chloramphenicol (Fisher), 50 μg/ml kanamycin sulfate (Jersey Lab Supply), and 500 μg/ml erythromycin (Fisher) as appropriate.

Mutant construction. All oligonucleotide sequences used in plasmid construction are given in Table S1 in the supplemental material. In order to create plasmid insertion mutations, truncated forms of each gene, containing the ribosome binding site but lacking a promoter, were generated using PCR as previously described (11). The truncated form of *sleB* contained 135 codons of the 305-codon gene. The *cwlJ1* and *cwlJ2* truncations included 102 and 78 codons of their total 140 and 142 codons, respectively. The truncated gene fragments were recombined into pDONRtet and pNFd13 (11) by using the Gateway cloning system (Invitrogen), and the resulting plasmids were inserted into the *B. anthracis* chromosome as described previously (11). PCR was used to confirm the gene disruptions. These plasmid insertions also created transcriptional fusions to *lacZ* (11).

In order to create in-frame deletions of each gene, PCR was used to amplify the entire target gene as well as several hundred bases up- and downstream. Each fragment was cloned into pBKJ236 (17) by using the corresponding endonucleases. Inverse PCR with appropriate primers produced deletion constructs with BglI sites at the deletion points, and BglI digestion and subsequent ligation were used to create plasmids carrying in-frame deletions. The *sleB* deletion eliminated all but the first 10 and the last 9 codons of the gene. The *cwlJ1* and *cwlJ2* deletions left only the first three and last two codons of each gene. Each mutation was introduced into *B. anthracis* via markerless gene replacement as previously described (17). Complementation of each mutation was achieved by introduction of the pBKJ236 derivative with the corresponding full-length gene, while empty pBKJ236 served as a negative control. These complementing plasmids were maintained extrachromosomally at the permissive temperature of 27°C and under erythromycin selection.

β-Galactosidase assay. Strains carrying *lacZ* fusions were grown in Mod G medium, and samples were taken during sporulation, concomitantly with optical density (OD) readings. Cell samples were permeabilized with 2% CHCl$_3$ and 0.001% sodium dodecyl sulfate, and β-galactosidase activity was determined using the substrate *o*-nitrophenyl-β-D-galactopyranoside as previously described (27).

Germination assays. Spore germination and outgrowth were assayed by changes in OD$_{600}$ over time. Synchronous germination was achieved by heat activating spores at 70°C for 20 min and then suspending them in BHI broth to an OD$_{600}$ of 0.2 at 39°C. Spore viability was determined using a simple plating assay in which spores were first germinated in BHI. Germination and outgrowth to 100% of the initial OD$_{600}$ were carried out to reduce spore aggregation, followed by serial dilution and plating. Number of CFU per OD$_{600}$ unit was

TABLE 2. Homologs of *B. subtilis* GSLEs

B. subtilis protein		*B. anthracis* homolog[a]			%[b]	
Name	Size (no. of amino acids)	Name	Locus	Size (no. of amino acids)	Identity	Similarity
SleB	305	SleB	BAS2562	253	53	67
CwlJ	142	CwlJ1	BAS5241	140	62	76
		CwlJ2	BAS2417	142	58	76
SleL (YaaH)	427	SleL	BAS3402	430	48	70

[a] Homolog names are based on homologous proteins in *B. subtilis* and are unique for the purposes of this research.
[b] The percentages of amino acid identity and similarity were determined using BLASTP 2.2.18 (31, 44).

calculated after incubation overnight at 39°C. Release of DPA and cortex fragments during germination in buffer was assayed as previously described (10). When required, the coats of *B. anthracis* spores were permeabilized (decoated) as previously described (36).

HPLC analysis of PG. Spores were germinated in buffer and used to prepare PG for reverse-phase high-performance liquid chromatography (RP-HPLC) analysis as previously described (10). Briefly, the germinated spore suspension was separated into spore-associated (pellet) and released-exudate (supernatant) fractions. Lytic enzymes were inactivated with heat (supernatant) or with heat and detergent (pellet), and PG was purified. The PG material from the pellets and half of each exudate fraction were then digested with the muramidase mutanolysin (Sigma). All fractions were reduced with $NaBH_4$ prior to HPLC separation.

Amino acid-and-sugar analysis was used to characterize novel muropeptides eluted from the HPLC separation. The phosphate buffer from each collected muropeptide was removed by repeating the HPLC separation in 0.05% trifluoroacetic acid with a 0 to 20% acetonitrile gradient. The novel compounds were then hydrolyzed in HCl vapor and analyzed as previously described (10). Muropeptides of interest were identified by mass spectrometry using an Applied Biosystems 3200 Q Trap tandem mass spectrometry system. The total mass and fragmentation of each compound in the negative-ion mode were determined as previously described (35).

RESULTS

GSLE homologs in *B. anthracis*. Analysis of sequence similarities suggested that *B. anthracis* contains GSLE homologs in its genome (Table 2). The most notable of these are one homolog of SleB and two homologs of CwlJ. A second *B. anthracis* homolog of SleB is more closely related to another *B. subtilis* cell wall hydrolase, YkvT, which plays no role in spore metabolism (8, 15). For this reason, the second homolog of SleB was not analyzed. No homologs of the *Clostridium perfringens* SleC or SleM (7, 28) GSLEs were identified in the *B. anthracis* genome.

In *B. subtilis*, *sleB* is the first gene in a bicistronic operon with *ypeB*. Interestingly, the *sleB* homolog at locus BAS2562 in *B. anthracis* appears to be the first in a putative tricistronic operon. The second open reading frame, BAS2561, is homologous to *ypeB*. The product of the third open reading frame in this possible operon shares homology with the uncharacterized *B. subtilis* protein YlaJ (22).

The *B. anthracis* *cwlJ* homolog at locus BAS5241 is the first in a putative bicistronic operon with a *gerQ* homolog at BAS5242. The second *cwlJ* homolog, at BAS2417, appears to be monocistronic. For the duration of this correspondence,

BAS5241 and BAS2417 will be referred to as *cwlJ1* and *cwlJ2*, respectively, and the gene at BAS2562 will be called *sleB*.

GSLE-encoding genes are transcribed during sporulation. Plasmid insertion mutagenesis allowed the investigation of gene expression through the resulting genetic fusion of *lacZ* to the native promoter of each GSLE-encoding gene. Expression from these promoters was monitored by assaying β-galactosidase activity. The start of sporulation was defined as the transition from growth into stationary phase as observed by change in OD_{600} and is termed time zero (t_0). Wild-type *B. anthracis*, without a *lacZ* fusion, exhibited the lowest levels of β-galactosidase activity throughout the experiment (Fig. 1A and B). The highest level of activity was produced by the *cwlJ1* fusion, starting about 1 hour after sporulation initiation (t_1). The transcription of *cwlJ1* peaked near $t_{3.5}$, which also coincided with the maximum activity for the *sleB* and *cwlJ2* fusions. However, the expression levels of both the *cwlJ2* and the *sleB* promoters were markedly lower and were not detectable above the background prior to $t_{2.5}$ (Fig. 1B). The peak *cwlJ2* and *sleB* expression levels were 5- to 10-fold above background, similar to
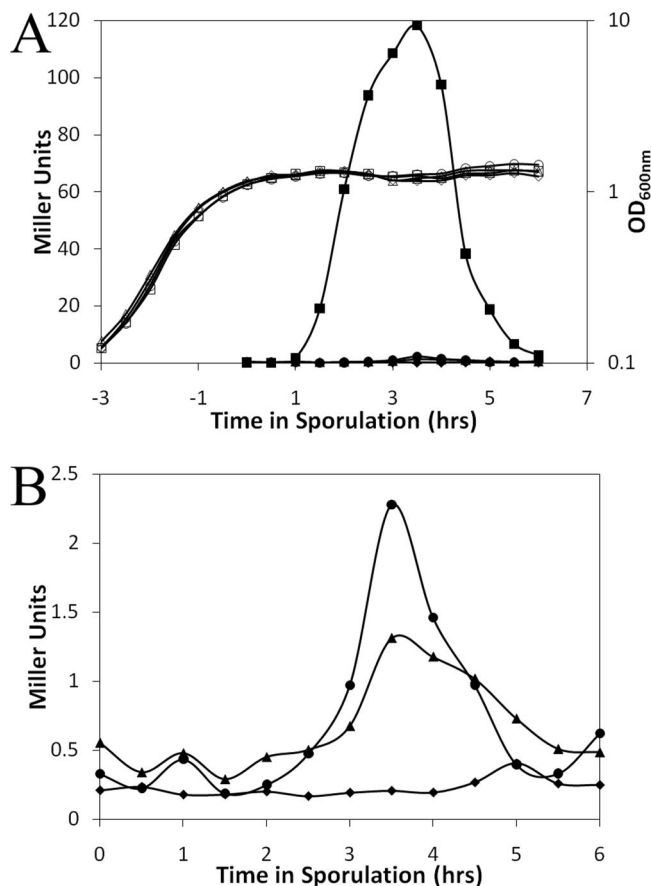

FIG. 1. Expression of *cwlJ1*, *cwlJ2*, and *sleB* during *B. anthracis* sporulation. Strains carrying each promoter-*lacZ* fusion were shaken in Mod G medium at 39°C and were assayed for β-galactosidase activity. (A) OD (open symbols) and β-galactosidase activity (filled symbols) are shown for a wild-type strain lacking *lacZ* (◆) and for strains with *lacZ* fused to *cwlJ1* (■), *cwlJ2* (▲), and *sleB* (●). (B) β-Galactosidase activity for the wild type, *cwlJ2-lacZ*, and *sleB-lacZ* are shown on an expanded *y* axis for clarity. Both panels show representative data for one of three independent experiments.
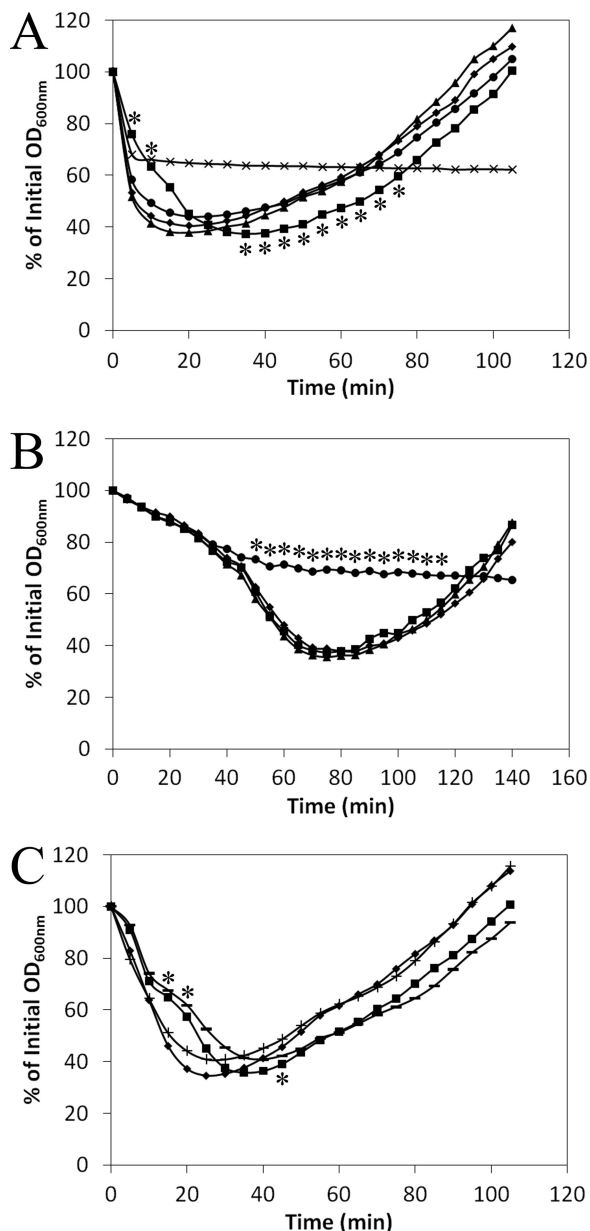
FIG. 2. Germination and outgrowth of native and decoated spores in BHI. Wild-type (♦), cwlJ1 and ΔcwlJ1 (■), cwlJ2 (▲), sleB (●), ΔcwlJ1 ΔsleB (✕), ΔcwlJ1-plus-pBKJ236 (−), and ΔcwlJ1-plus-pDPV345 (+) spores were heat activated and germinated in BHI at 39°C. (A) Germination of native spores. (B) Germination of decoated spores. (C) Complementation of the ΔcwlJ1 phenotype. Data shown are averages for three independent experiments; error bars are omitted for clarity. Asterisks indicate those time points when cwlJ1 (A), sleB (B), or ΔcwlJ1 and ΔcwlJ1-plus-pBKJ236 (C) spores were significantly different (P ≤ 0.05) from wild-type spores. The ΔcwlJ1 ΔsleB spores (A) were significantly different from those of the wild type at all time points except 60 to 70 min, where the lines cross.

those observed for germinant receptors with the same type of lacZ fusion (11).

Our expression results agree with earlier microarray and proteome investigations of B. anthracis that suggest that cwlJ1 is expressed during an early wave of sporulation-associated transcription, which is then followed closely by another wave,

which includes sleB (4, 21). This is further supported by our observation of candidate promoter sequences for σ^E and σ^G (13) upstream of cwlJ1 and sleB, respectively (data not shown). The observed time for cwlJ2 expression in this work more closely matches that for sleB than it does that for cwlJ1.

Effects of GSLE mutations on germination. None of the single- or double- mutant strains exhibited any significant deviations from the wild type with regard to doubling time during exponential growth, formation of heat-resistant spores, or spore morphology (data not shown).

Spores of strains lacking cwlJ1, cwlJ2, sleB, or both cwlJ1 and sleB were germinated in BHI and monitored through germination and outgrowth by measuring the change in OD_{600}. As spores germinate, they rapidly lose between 40% and 60% of their OD within the first few minutes of contact with germinants. This is due to spore water uptake, Ca-DPA release, and cortex hydrolysis (34). As the spore population completes germination and enters outgrowth, the OD_{600} increases, thus continuing into vegetative growth.

Native spores of wild-type and all single mutant strains lost at least 58% of their initial ODs, indicating that all were successful at synchronous germination (Fig. 2A). However, the precise kinetics for strains to finish germination and enter outgrowth was variable. The cwlJ2 and sleB mutants mimicked the wild type in their progress and lost 40% of their initial ODs within 1 minute of each other. The entire curve for cwlJ2 spores looked almost identical to that for the wild type, but the sleB spores appeared to undergo a slightly less efficient germination response, coupled with a lower rate of outgrowth. Due to variability among spore preparations, this slow response of sleB spores was not statistically different from that of wild-type spores, but it was reproducible in three independent spore preparations.

An overall delay by cwlJ1 spores was evident by the rightward shift of the strain's germination curve. Compared to the wild type, cwlJ1 spores were significantly delayed in OD loss from 5 to 10 minutes after germination initiation as well as during outgrowth for a span of 40 minutes (P ≤ 0.05, as determined by an unpaired Student t test) (Fig. 2A). These spores took at least twice as long as wild-type spores to lose 40% of their starting OD (Table 3), and the time it took to reach their minimal OD was also significantly delayed. The

TABLE 3. Germination of spores in BHI[a]

Genotype	Native spores		Decoated spores	
	Time for 40% loss of OD[b] (min)	No. of CFU/ OD unit	Time for 40% loss of OD[b] (min)	No. of CFU/ OD unit
Wild type	4 ± 1	1×10^8	54 ± 10	1×10^8
cwlJ1	14 ± 5*	1×10^8	54 ± 5	1×10^8
cwlJ2	4 ± 1	1×10^8	53 ± 8	1×10^8
sleB	5 ± 2	9×10^7	NA	1×10^5*
cwlJ1 sleB	NA	1×10^5*	NT	NT

[a] Averages were determined from three independent experiments. NA, not applicable (the sample never reached a 40% loss); NT, not tested. * indicates a value that is significantly different from those for similarly treated wild-type spores, with P values of ≤ 0.01, as determined by an unpaired two-tailed Student t test.
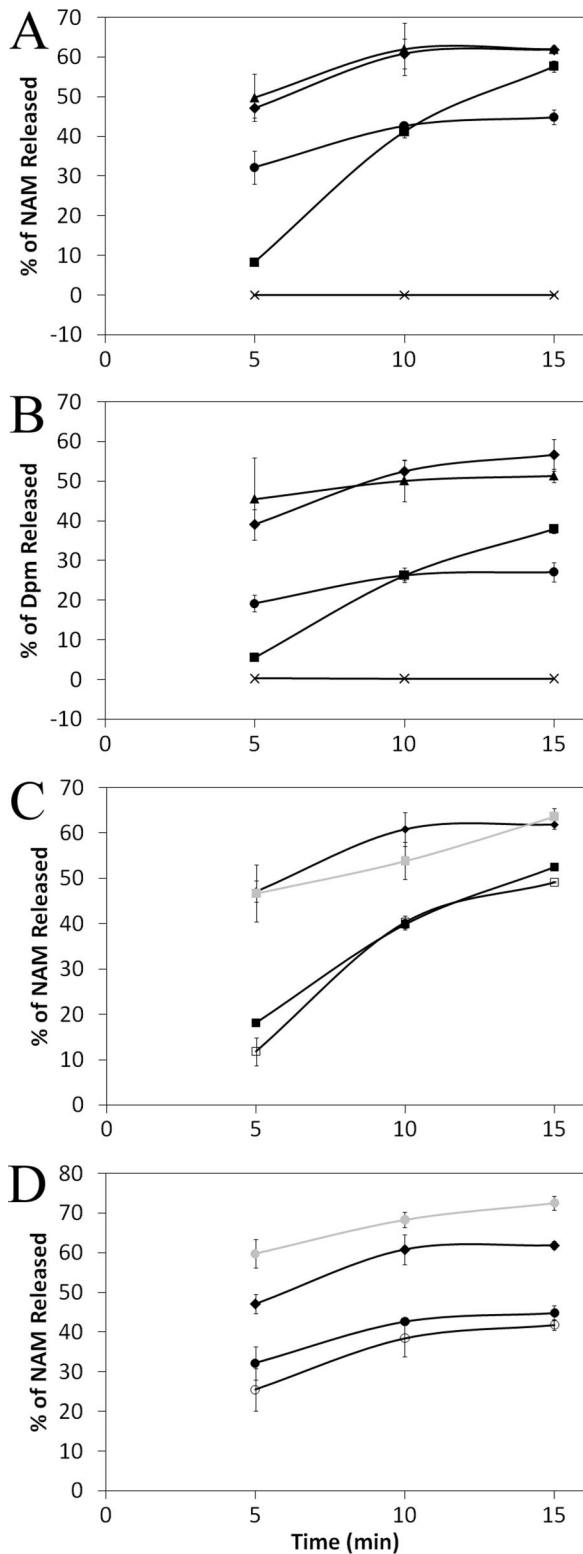[b] Values are rounded to the nearest minute. The error is 1 standard deviation from the mean.

FIG. 3. Release of NAM and Dpm from germinating *B. anthracis* spores. Dormant wild-type (◆), *cwlJ1* (■), *cwlJ2* (▲), *sleB* (●), and Δ*cwlJ1* Δ*sleB* (×) spores in buffer were germinated with L-alanine and inosine and were sampled for the release of NAM (A) and Dpm (B) at 5-minute intervals after contact with germinants. (C) Complementation of Δ*cwlJ1* (■) NAM release was tested with Δ*cwlJ1*(pDPV345) (▨) and Δ*cwlJ1*(pBKJ236) (□) spores. (D) Complementation of Δ*sleB* (black circles) NAM release was tested with Δ*sleB*(pDPV346) (gray

rate of outgrowth for the *cwlJ1* strain was normal; its starting point was simply delayed due to slowed germination. Identical effects on germination were obtained with plasmid insertion and in-frame deletion mutations in each gene (data not shown), suggesting that if other genes in these operons play significant roles in germination, then they may be involved in the same GSLE functions. The *cwlJ1* slow-germination phenotype was complemented with pDPV345 but not the empty-vector control (Fig. 2C).

Spores produced by the *cwlJ1 sleB* double deletion strain were capable of losing OD only in the first 5 minutes after contact with germinants (Fig. 2A). Germination was arrested at this point, and a 40% loss in OD was never reached (Table 3), nor was the OD ever observed to increase (Fig. 2A). This defect was complete enough to affect spore viability since the Δ*cwlJ1* Δ*sleB* spores had a 1,000-fold loss in colony-forming ability (Table 3). Native spores lacking only one of the putative GSLEs had no change in viability.

Permeabilizing (decoating) the spore coats either removes or greatly disrupts proteins sequestered in that region of the spore (36). In *B. subtilis*, CwlJ and SleL have been shown to be located in or near the coat of dormant spores while SleB localizes to the cortex or membrane layers (8, 19, 39). As such, decoating spores offered a logical avenue for determining the effects of simultaneously losing the functions of three putative GSLEs (CwlJ1, CwlJ2, and SleL), as shown in *B. subtilis* (36). For each strain, the germination of decoated spores was substantially delayed compared to that of untreated spores (Table 3). Regardless, the stages of germination (loss of OD_{600}) and outgrowth (increase in OD_{600}) remained apparent and synchronous for wild-type, *cwlJ1*, and *cwlJ2* strains (Fig. 2B). The fact that decoated wild-type and *cwlJ1* spores act indistinguishably suggests that this treatment inactivated CwlJ1.

The most profound result from investigating decoated spores was revealed by the *sleB* mutant. These spores responded to nutrients and engaged in early germination events indistinguishably from the wild type (Fig. 2B). However, that progress was arrested at a point just prior to loss of 25% of the initial OD. From this point on, any loss of OD occurred at a significantly lower rate ($P \leq 0.05$). Decoated *sleB* spores never reached a 40% loss of OD or exhibited any characteristics of outgrowth. Continued observation revealed no further loss in OD over 4.5 h (data not shown). The decoating treatment did not prevent wild-type, *cwlJ1*, or *cwlJ2* spores from germinating and forming colonies. However, the decoated *sleB* spores had a 1,000-fold loss in colony forming ability. This was not simply a long germination delay; continued observation of plates for 3 days revealed no new colony appearance. It should be noted that this phenotype is identical to what was observed for native *cwlJ1 sleB* double mutant spores.

DPA, NAM, and Dpm release from spores. One of the earliest events in spore germination is the release of Ca-DPA from the spore core into the surrounding medium (23). De-

circles) and Δ*sleB*(pBKJ236) (white circles) spores. All error bars represent 1 standard deviation from the mean for three (A, B, and D) or two (C) independent experiments. All points have error bars, but in some cases, these are too small to be visible.

TABLE 4. Muropeptide peak identification

Monopeptide source and name[a]	Structure[b]	Source[c]
Dormant-spore peptidoglycan		
A	DS-TriP	
B	DS-Ac-TriP	Germ cell well
C	DS-TriP+Am	Germ cell well
D	DS-Ac-TriP+Am	Germ cell well
E	DS-Ala	
F	DS-TP	
G	DS-Ac-TP	
H	TS-TP open lactam	Cortex
I	TS Red-TP	Cortex
J	TS Red-Ala	Cortex
K	DS-Ac-TP x TriP+Am-DS-Ac	Germ cell well
L	TS-TP-Ac	Cortex
M	DS-Ac-TP+Am x TriP+Am-DS-Ac	Germ cell well
N	TS-TP	Cortex
O	TS-TP x TP	Cortex
P	DS-TP x TP-TS Red	Cortex
Q	TS-Ala	Cortex
R	HS Red-Ac-TP (right lactam reduced)	Cortex
S	HS Red-Ac-TP (left lactam reduced)	Cortex
T	DS-TP x TP-TS	Cortex
U	HS-TP-Ac	Cortex
V	TS-TP x TP-TS	Cortex
W	HS-Ala-Ac	Cortex
X	HS-Ala-Ac	Cortex
Y	HS-TP	Cortex
Z	HS-Ala	Cortex
AA	TS-TP x TP-HS	Cortex
Germinated spore exudate		
Following Mutanolysin digestion		
aG1	TriS-TP Red	Cortex, N-acetylglucosaminidase
aG4	TriS-TP	Cortex, N-acetylglucosaminidase
aG5	TriS-Ala	Cortex, N-acetylglucosaminidase
aG8	PS-TP-Ac	Cortex, N-acetylglucosaminidase
Without Mutanolysin digestion		
aG2	TS-TP NAGr Red	Cortex, N-acetylglucosaminidase
aG3	TS-Ala NAGr Red	Cortex, N-acetylglucosaminidase
aG6	TS-TP NAGr	Cortex, N-acetylglucosaminidase
aG7	TS-Ala NAGr	Cortex, N-acetylglucosaminidase
aG7a	TS-TP anhydro	Cortex, lytic transglycosylase
aG7b	TS-Ala anhydro	Cortex, lytic transglycosylase
aG10u	HS-TP-Ac NAGr	Cortex, N-acetylglucosaminidase
aG12	HS-Ala-Ac NAGr	Cortex, N-acetylglucosaminidase

[a] Muropeptide names are determined by their order of elution during RP-HPLC. Muropeptide names preceded by "a" indicate those generated by *B. anthracis* in order to differentiate them from those generated by other species.
[b] Abbreviations: DS, disaccharide (NAG-NAM); TS, tetrasaccharide (NAG-lactam-NAG-NAM); HS, hexasaccharide (NAG-lactam-NAG-lactam-NAG-NAM); TriS, trisaccharide (lactam-NAG-NAM); PS, pentasaccharide (lactam-NAG-lactam-NAG-NAM); TriP, tripeptide (Ala-Glu-Dpm); TP, tetrapeptide (Ala-Glu-Dpm-Ala); Ac, deacetylated glucosamine; +Am, amidated Dpm; Red, reduced lactam (an artifact of sample preparation (43)); NAGr, NAG at the reducing end; x, cross-link between two peptides. "Anhydro" indicates that the NAM at the reducing end is in the anhydro form.
[c] The structure of origin for each muropeptide is shown, under the assumptions that muramic-δ-lactam is unique to the cortex and that tripeptide is exclusive to the germ cell wall. Entries that are blank indicate that the muropeptide cannot be attributed to a single source. For muropeptides released during germination, the enzymatic activity responsible is indicated.

spite observed changes in OD loss during germination, all of the mutant spores, including those of the *cwlJ1 sleB* double mutant, released as much DPA as the wild type during the earliest minutes following exposure to germinants (data not shown). In order to assay for the later steps in the germination process, one can analyze the ratio of the cortex-specific components NAM and Dpm found in the pellet versus the exudate fractions of germinating spores. Release of these compounds is rapid under the conditions used for this assay, with measurable differences over the course of a few minutes (10). Assays re-

vealed that both wild-type and *cwlJ2* spores released ~50% of their NAM and Dpm within the first 5 minutes of contacting germinants, with maximum release occurring by 10 minutes (Fig. 3A and B).

cwlJ1 spores were incapable of releasing cortex components as rapidly; hence, after 5 minutes, only 8% and 6% of NAM and Dpm, respectively, had been released (Fig. 3A and B). Still, the cortex was swiftly released from the *cwlJ1* spores in the following minutes and approached the wild-type release level by 15 minutes. This result coincides with the delay in

Pellet
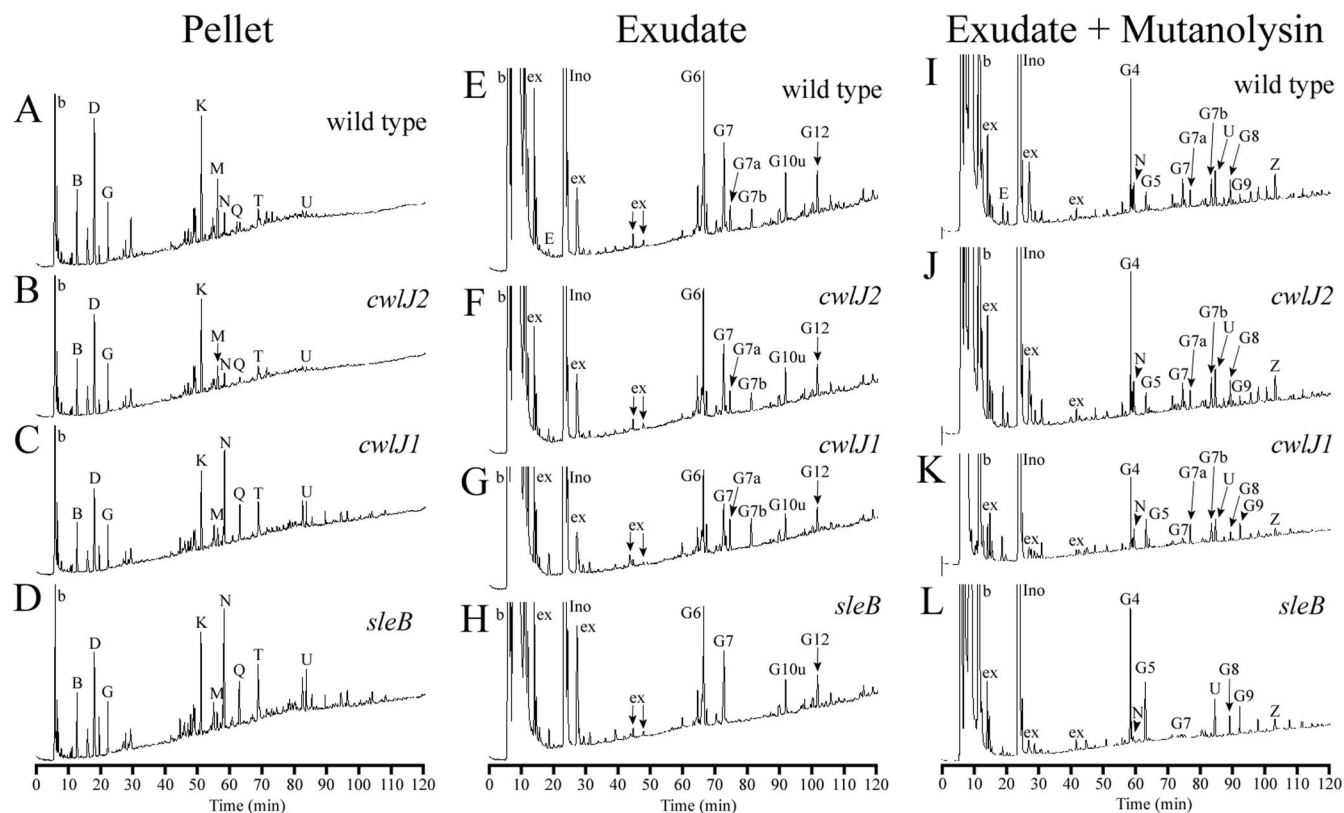

Exudate

Exudate + Mutanolysin

FIG. 4. RP-HPLC separation of muropeptides from germinating *B. anthracis* spores. PG was prepared from germinating spore suspensions as described in Materials and Methods. Samples were collected after spore suspensions had lost 40% of their initial ODs: approximately 5 min for wild-type and *cwlJ2* spores and 10 min for *cwlJ1* and *sleB* spores. PG from germinating spore pellets (A to D) and from 50% of the exudate preparations (I to L) were digested with muramidase, reduced, and separated as previously described (26). The other 50% of the exudates (E to H) were reduced and separated without muramidase digestion. Peaks are numbered as in reference 10 and in Table 4, but the initial "a" in the germination-specific-peak names were omitted for space considerations. Early-eluting peaks labeled "b" are buffer components present in blank samples. Peaks labeled "ex" are spore exudate components that, based upon amino acid analysis, are not derived from PG. Peaks labeled "Ino" are from the inosine used to germinate spores.

germination response revealed by OD changes (Fig. 2A). Complementation with pDPV345, but not with the vector control, restored both NAM and Dpm release to wild-type levels (Fig. 3C and data not shown).

Spores without *sleB* were also delayed in discharging their cortex, despite having no obvious changes in OD loss (Fig. 2A and 3A and B). Initially, the delay was not as dramatic as that exhibited by the *cwlJ1* spores; however, over the following minutes, the *sleB* mutant did not release cortex as speedily, thus resulting in the least total release among all single-mutant strains. Fifteen minutes after the start of germination, *sleB* spores had managed to release only 45% and 27% of their total NAM and Dpm, respectively. Complementation with pDPV346, but not with the vector control, restored both NAM and Dpm release to wild-type levels (Fig. 3D and data not shown). Deleting both *cwlJ1* and *sleB* resulted in spores that released no NAM or Dpm during germination (Fig. 3A and B).

Cortex hydrolysis is slowed in *cwlJ1* and *sleB* spores. Previous HPLC analyses revealed that wild-type *B. anthracis* spores released the majority of their cortex within the first 10 minutes of germination with L-alanine and inosine (10). We obtained similar results, where after 5 min of germination, muropeptides derived from the spore pellet were predominantly germ

cell wall associated (for example, peaks K and M) (Table 4 and Fig. 4A), and all of the PG fragments found in germinating spore exudates were derived from the cortex (Table 4 and Fig. 4E and I). When *cwlJ2* was disrupted, the chromatograms of pellet and exudate fractions were indistinguishable from those of the wild type (Fig. 4B, F, and J).

Spores lacking *cwlJ1* did not release muropeptides nearly as well. In fact, *cwlJ1* spores retained so much more spore PG during germination that cortex-derived muropeptides became the dominant peaks in the chromatogram of spore-associated material (for example, peaks N and Q) (Fig. 4C). The average amount of muropeptide N retained increased by >350% when *cwlJ1* was disrupted. This retention of cortex was coupled with a decrease in cortex release, as seen in exudates of germinating spores (Fig. 4G and K). Cortex-derived muropeptides G6 and G7 diminished from levels seen in wild-type spore exudates by averages of 48% and 50%, respectively (Fig. 4E and G). The same change was observed when exudates were digested with mutanolysin, except G4, the product of mutanolysin activity on G6, was subject to a decrease (Fig. 4I and K). A previous analysis of cortex hydrolysis by a *B. subtilis cwlJ* mutant revealed no change relative to the wild-type level (8). This difference is likely due to the very slow release of muropeptides
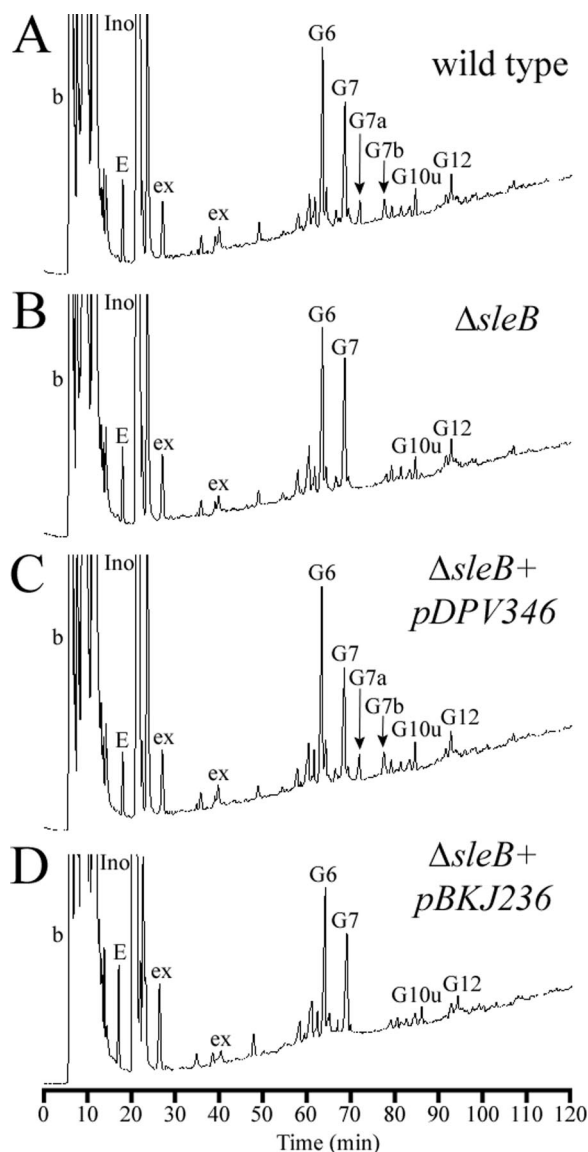
FIG. 5. Complementation of Δ*sleB*. Samples were prepared and analyzed, and peaks are labeled, as described for Fig. 4. (A) Muropeptides released from wild-type spores. (B) Muropeptides released from Δ*sleB* spores. (C) Muropeptides released from spores with Δ*sleB* plus the complementing plasmid pDPV346. (D) Muropeptides released from spores with Δ*sleB* plus the control vector pBKJ236.
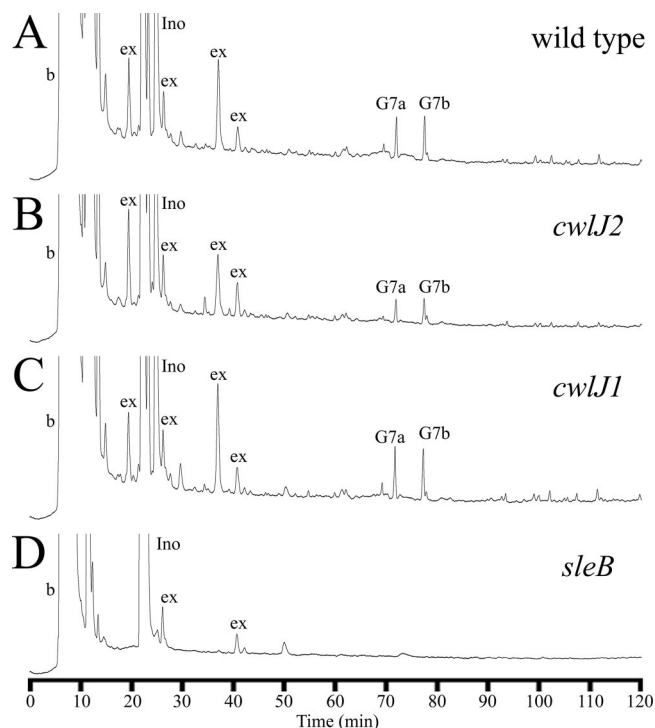

FIG. 6. RP-HPLC separation of muropeptide exudates from decoated germinating *B. anthracis* spores. Spores were permeabilized as previously described (36). Samples were prepared and analyzed, and peaks are labeled, as described for Fig. 4. All samples were harvested after spores lost 40% of their initial OD (~45 min). (A) Muropeptides released from wild-type spores. (B) Muropeptides released from *cwlJ2* spores. (C) Muropeptides released from *cwlJ1* spores. (D) Muropeptides released from *sleB* spores.

by *B. subtilis*, relative to that by *B. anthracis* (10), making a difference in relative rate of release by *B. subtilis* strains difficult to detect.

Spores lacking SleB also exhibited a defect in muropeptide release. Much more cortex remained in the spore during germination; for instance, muropeptide N had an average increase of >350% compared to the wild-type level (Fig. 4D). This result is nearly identical to what was seen in *cwlJ1* spores; however, the associated change in released muropeptides was unique. The exudates of *sleB* spores did not contain any of the G7a or G7b muropeptides (Fig. 4H). Exudate digested with mutanolysin lacked the same two muropeptides (Fig. 4L), but no other muropeptides were altered from what was observed in

wild-type exudates. This phenotype was fully complemented by introducing *sleB* on a plasmid but not by the empty vector (Fig. 5A to D). The requirement for SleB in the production of this class of anhydromuropeptide (see below) was also observed in *B. subtilis* (5). No muropeptides were released from spores containing both the *cwlJ1* and the *sleB* deletions (data not shown). The germinated spore pellets contained cortex identical to that found in dormant *B. anthracis* spores during previous work (10).

Spores that had been decoated were also poor at digesting cortex. Pellet fractions of these spores contained the majority of total PG as N replaced K as the dominant peak (data not shown). Very little material was released in the exudates (Fig. 6A to D). Decoated wild-type, *cwlJ1*, and *cwlJ2* spores all generated similar exudate muropeptide profiles. Prior to mutanolysin exposure, the predominant muropeptides were G7a and G7b. After treatment with mutanolysin, G7a and G7b remained, but N was the dominant muropeptide (data not shown), indicating that the exudates contained large, not fully digested PG fragments. Decoated *sleB* spores, similarly to the *sleB cwlJ1* double mutant under native conditions, released little to no PG during germination, with or without mutanolysin digestion (Fig. 6D and data not shown).

Muropeptides G7a and G7b contain anhydromuramic acid. Muropeptides G7a and G7b were identified through a combination of amino acid analysis and mass spectrometry (Fig. 7
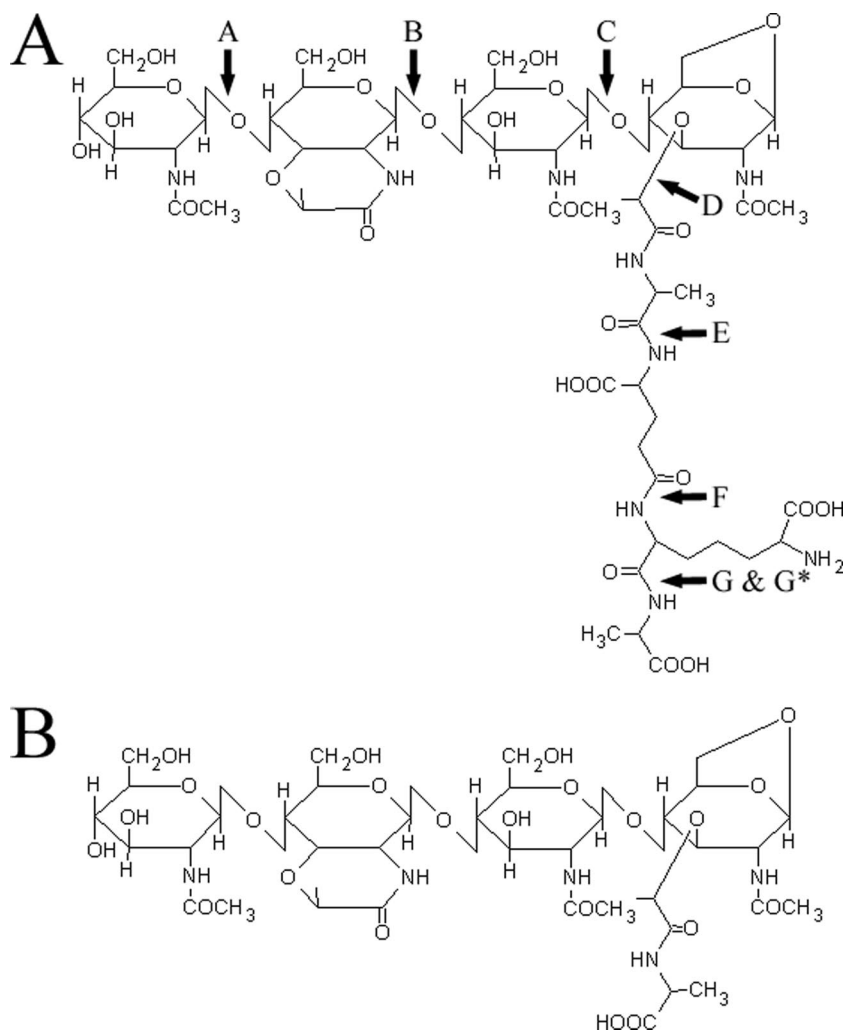
FIG. 7. Muropeptide J1 and J2 are anhydro-tetrasaccharides. Structures were determined with a combination of HPLC amino acid/sugar analysis and electrospray ionization-mass spectrometry. (A, B) The sugar residues are (from left to right) NAG, muramic-δ-lactam, NAG, and anhydro-NAM. (A) The amino acid residues are (in order from lactyl linkage) L-alanine, D-glutamate, meso-diaminopimelic acid, and D-alanine. Arrows indicate sites of fragmentation during electrospray ionization-mass spectrometry, as identified in Table 5. (B) The single-amino-acid side chain is L-alanine.

and Table 5). The ratio of individual amino acids in G7a matched the expectations for a muropeptide containing a tetrapeptide side chain. The qualitative results of an amino sugar analysis revealed that only NAM and NAG were present. No reduced sugars, muramitol (MOH) or glucosaminitol, were detected, despite the fact that the sample was reduced prior to HPLC separation, indicating that the "reducing-end" sugar in this muropeptide is resistant to reduction. Mass spectrometry showed G7a to be 20 Da smaller than the tetrasaccharide-tetrapeptide muropeptide N (Table 4). N releases MOH upon amino sugar analysis due to the reduction prior to HPLC separation (10). If G7a is ordered similarly to a TS-TP, then the 20-Da mass discrepancy can be explained by the presence of an anhydromuramic acid as the product of a lytic transglycosylase (2, 14). Mass spectrometry analysis of G7a fragmentation exactly matches the expectations of anhydro-tetrasaccharide tetrapeptide (Table 5 and Fig. 7). Amino acid analysis, mass spectrometry, and fragmentation analysis of muropeptide

G7b (Table 5 and data not shown) revealed that it is anhydro-tetrasaccharide alanine.

DISCUSSION

The GSLE mechanism of *B. anthracis* spores appears to function similarly to that of *B. subtilis*, with some minor but potentially important differences. *B. anthracis* strains with mutations affecting *cwlJ1*, *cwlJ2*, *sleB*, or *cwlJ1* and *sleB* grow, divide, and sporulate without difficulty, and their spores initially respond normally to nutrient germinants. In *B. subtilis*, the germination muropeptide profiles of wild-type and *cwlJ* spores are indistinguishable (8), but for *B. anthracis*, we were able to observe significantly fewer cortex-derived muropeptides being released from spores within 10 minutes after contacting germinants. The structures of the released muropeptides did not differ from those produced by the wild-type strain, leaving the bond specificity of any CwlJ1 enzymatic activity

TABLE 5. Novel muropeptide identification[a]

Group and name	Structure[b]	m/z[c]		Amino acid/amino sugar analysis[d]						
		Predicted	Observed	M	G	MOH	GOH	Ala	Glu	Dpm
aG7a	TS-TP anhydro	1,338.5	1,338.4	+	+	−	−	2	1	1
aG7b	TS-Ala anhydro	966.4	966.3	+	+	−	−	1	0	0
aG7a fragments[e]										
A	TriS-TP anhydro	1,135.5	1,135.2							
B	DS-TP anhydro	920.4	920.3							
C	MS-TP anhydro	717.3	717.2							
D	TS anhydro	823.3	823.1							
E	Glu-Dpm-Ala	389.2	389.2							
F	Dpm-Ala	260.1	260.2							
G	Ala	88.0	88.1							
G*	TS-TriP anhydro	1,251.6	1,251.2							

[a] Abbreviations: M, N-acetylmuramic acid; G, N-acetylglucosamine; GOH, glucosaminitol; TS, tetrasaccharide (NAG-ML-NAG-NAM); TriS, trisaccharide (ML-NAG-NAM); DS, disaccharide (NAG-NAM); MS, monosaccharide (NAM); TP, tetrapeptide (Ala-Glu-Dpm-Ala); TriP, tripeptide (Ala-Glu-Dpm); Ala, alanine; Glu, glutamate; Dpm, meso-diaminopimelic acid.
[b] Anhydro structures have a 1,6-anhydro linkage in the terminal NAM.
[c] Mass-to-charge ratio for the deprotonated ion of the predicted or expected muropeptide as determined by electrospray ionization-mass spectrometry.
[d] The analysis method does not allow reliable quantitative results for amino sugars. + indicates that the compound was clearly detected. − indicates that the compound was not clearly detected. For amino acids, the molar ratios are rounded to the nearest whole number.
[e] Fragment names refer to the muropeptide fragmentation indicated by arrows in Fig. 7.

unresolved. SleB, like CwlJ1, is required for timely cortex degradation, but its mode of action is unique. Two cortex fragments that are entirely dependent on SleB are the result of lytic transglycosylase activity. This activity was associated with SleB by using similar methods with *B. subtilis* but was not previously detected in *B. anthracis* (5, 10). In response to germinants, the *cwlJ1 sleB* double mutant spores initiate but are incapable of completing germination, similarly to *cwlJ sleB B. subtilis* spores (16). However, unlike for the situation in *B. subtilis*, we did not observe any delay in DPA release. The first 5 to 10 minutes of *B. anthracis* germination (~25% loss in OD) is independent of GSLE activity and includes the release of nearly all of the DPA. Very rapid DPA release, like quicker cortex fragment release (10), may be a function of thinner, more-permeable *B. anthracis* spore coat layers.

The highest rate of cortex degradation requires both *cwlJ1* and *sleB*, yet they do not cause release of cortex fragments in exactly the same manner (Fig. 3A and B). This suggests that SleB and CwlJ1 provide alternate pathways for cortex depolymerization (Fig. 8). We propose that this difference is best
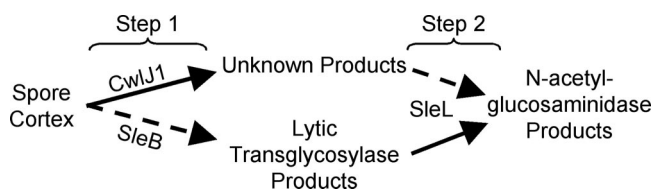

FIG. 8. Model for cortex hydrolysis by GSLEs in *B. anthracis*. The degradation of spore cortex is illustrated as two steps. Solid arrows indicate the reaction that is responsible for the majority of activity at that given step. Dashed arrows indicate those reactions that compose the minority of enzymatic activity. SleB and CwlJ1 are both capable of depolymerizing intact cortex, with more initial digestion due to CwlJ1. SleL, as a cortex fragment lytic enzyme, is capable of degrading only partially digested cortex. SleL prefers substrate provided by SleB, or the positioning of SleB results in production of a greater amount of SleL substrate. Fully digested cortex contains a mixed muropeptide population of all the shown substrates and products.

explained in context with SleL, which shares 98% identity with its *B. cereus* homolog and functions as an N-acetylglucosaminidase in both *B. anthracis* (20) and *B. cereus* (6). For *B. cereus*, SleL has been further defined as a cortex fragment lytic enzyme that recognizes only cortex substrate that has undergone previous digestion by another GSLE (6). In this model, the initial depolymerization of the cortex would be the responsibility of SleB and CwlJ1. The NAM release from a *cwlJ1* spore indicated that sixfold less cortex was digested and released than from wild-type spores in the first 5 minutes of germination (Fig. 3A). In addition, this was more than threefold less NAM than the *sleB* spores could discharge. These initial differences are likely due to a large disparity in protein available for depolymerization, as suggested by the higher level of *cwlJ1* transcription (Fig. 1A). However, this situation rapidly reverses as germination continues. Within 10 minutes, germinating *cwlJ1* and *sleB* spores have the same amount of NAM released, and by 15 minutes, *cwlJ1* spores have surpassed *sleB* spores to achieve NAM release at near-wild-type levels (Fig. 3A). It is our suggestion that the rapid acceleration of NAM release by *cwlJ1* spores is due to SleL action, which would have ample substrate available after several minutes of SleB-initiated cortex digestion. Meanwhile, *sleB* spores release cortex fragments early during germination due to naturally high levels of CwlJ1 but are unable to maintain this rapid release. Perhaps the population of cortex fragments that CwlJ1 yields does not provide the best substrate for SleL. Patterns of Dpm release support the same conclusions. Sequential digestion of spore PG by SleB and SleL has previously been suggested for *B. cereus* (24). Our model does not rule out the possibility that some number of CwlJ1-created muropeptides is acted on by SleL; indeed, SleL products are produced by *sleB* mutant spores. SleL may simply have a higher affinity for cortex fragments resulting from SleB action.

The responsibilities of *cwlJ1* and *sleB* are clearly redundant due to the partial effects on cortex lysis that they each have and the complete lysis defect that results when both are disrupted.

Further study of multiple mutant strains might provide novel muropeptide HPLC profiles that offer better insight into a specific lytic activity associated with *cwlJ1*. These studies should include *sleL* to provide a comprehensive analysis of the events during cortex degradation. Understanding the lytic germination activities that naturally diminish spore resistance can lead to methods that prematurely activate cortex degradation, thus greatly simplifying the process of cleaning *B. anthracis*-contaminated sites.

REFERENCES

1. **Atrih, A., and S. J. Foster.** 2001. In vivo roles of the germination-specific lytic enzymes of *Bacillus subtilis* 168. Microbiology **147:**2925–2932.
2. **Atrih, A., P. Zollner, G. Allmaier, M. P. Williamson, and S. J. Foster.** 1998. Peptidoglycan structural dynamics during germination of *Bacillus subtilis* 168 endospores. J. Bacteriol. **180:**4603–4612.
3. **Bagyan, I., and P. Setlow.** 2002. Localization of the cortex lytic enzyme CwlJ in spores of *Bacillus subtilis*. J. Bacteriol. **184:**1219–1224.
4. **Bergman, N. H., E. C. Anderson, E. E. Swenson, M. M. Niemeyer, A. D. Miyoshi, and P. C. Hanna.** 2006. Transcriptional profiling of the *Bacillus anthracis* life cycle in vitro and an implied model for regulation of spore formation. J. Bacteriol. **188:**6092–6100.
5. **Boland, F. M., A. Atrih, H. Chirakkal, S. J. Foster, and A. Moir.** 2000. Complete spore-cortex hydrolysis during germination of *Bacillus subtilis* 168 requires SleB and YpeB. Microbiology **146:**57–64.
6. **Chen, Y., S. Fukuoka, and S. Makino.** 2000. A novel spore peptidoglycan hydrolase of *Bacillus cereus*: biochemical characterization and nucleotide sequence of the corresponding gene, *sleL*. J. Bacteriol. **182:**1499–1506.
7. **Chen, Y., S. Miyata, S. Makino, and R. Moriyama.** 1997. Molecular characterization of a germination-specific muramidase from *Clostridium perfringens* S40 spores and nucleotide sequence of the corresponding gene. J. Bacteriol. **179:**3181–3187.
8. **Chirakkal, H., M. O'Rourke, A. Atrih, S. J. Foster, and A. Moir.** 2002. Analysis of spore cortex lytic enzymes and related proteins in *Bacillus subtilis* endospore germination. Microbiology **148:**2383–2392.
9. **Cowan, A. E., D. E. Koppel, B. Setlow, and P. Setlow.** 2003. A soluble protein is immobile in dormant spores of *Bacillus subtilis* but is mobile in germinated spores: implications for spore dormancy. Proc. Natl. Acad. Sci. USA **100:**4209–4214.
10. **Dowd, M. M., B. Orsburn, and D. L. Popham.** 2008. Cortex peptidoglycan lytic activity in germinating *Bacillus anthracis* spores. J. Bacteriol. **190:**4541–4548.
11. **Fisher, N., and P. Hanna.** 2005. Characterization of *Bacillus anthracis* germinant receptors in vitro. J. Bacteriol. **187:**8055–8062.
12. **Hanna, P. C., and J. A. Ireland.** 1999. Understanding *Bacillus anthracis* pathogenesis. Trends Microbiol. **7:**180–182.
13. **Helmann, J. D., and C. P. Moran, Jr.** 2001. RNA polymerase and sigma factors, p. 289–312. *In* A. L. Sonenshein, J. A. Hoch, and R. Losick (ed.), *Bacillus subtilis* and its close relatives: from genes to cells. American Society for Microbiology, Washington, DC.
14. **Höltje, J. V., D. Mirelman, N. Sharon, and U. Schwarz.** 1975. Novel type of murein transglycosylase in *Escherichia coli*. J. Bacteriol. **124:**1067–1076.
15. **Howell, A., S. Dubrac, K. K. Andersen, D. Noone, J. Fert, T. Msadek, and K. Devine.** 2003. Genes controlled by the essential YycG/YycF two-component system of Bacillus subtilis revealed through a novel hybrid regulator approach. Mol. Microbiol. **49:**1639–1655.
16. **Ishikawa, S., K. Yamane, and J. Sekiguchi.** 1998. Regulation and characterization of a newly deduced cell wall hydrolase gene (*cwlJ*) which affects germination of *Bacillus subtilis* spores. J. Bacteriol. **180:**1375–1380.
17. **Janes, B. K., and S. Stibitz.** 2006. Routine markerless gene replacement in *Bacillus anthracis*. Infect. Immun. **74:**1949–1953.
18. **Kim, H. U., and J. M. Goepfert.** 1974. A sporulation medium for *Bacillus anthracis*. J. Appl. Bacteriol. **37:**265–267.
19. **Lai, E. M., N. D. Phadke, M. T. Kachman, R. Giorno, S. Vazquez, J. A. Vazquez, J. R. Maddock, and A. Driks.** 2003. Proteomic analysis of the spore coats of *Bacillus subtilis* and *Bacillus anthracis*. J. Bacteriol. **185:**1443–1454.
20. **Lambert, E. A., and D. L. Popham.** 2008. The *Bacillus anthracis* SleL (YaaH) protein is an *N*-acetylglucosaminidase involved in spore cortex depolymerization. J. Bacteriol. **190:**7601–7607.
21. **Liu, H., N. H. Bergman, B. Thomason, S. Shallom, A. Hazen, J. Crossno, D. A. Rasko, J. Ravel, T. D. Read, S. N. Peterson, J. Yates III, and P. C. Hanna.** 2004. Formation and composition of the *Bacillus anthracis* endospore. J. Bacteriol. **186:**164–178.
22. **Mäder, U., G. Homuth, C. Scharf, K. Büttner, R. Bode, and M. Hecker.** 2002. Transcriptome and proteome analysis of *Bacillus subtilis* gene expression modulated by amino acid availability. J. Bacteriol. **184:**4288–4295.
23. **Magge, A., A. C. Granger, P. G. Wahome, B. Setlow, V. R. Vepachedu, C. A. Loshon, L. Peng, D. Chen, Y. Q. Li, and P. Setlow.** 2008. Role of dipicolinic acid in the germination, stability, and viability of spores of *Bacillus subtilis*. J. Bacteriol. **190:**4798–4807.
24. **Makino, S., and R. Moriyama.** 2002. Hydrolysis of cortex peptidoglycan during bacterial spore germination. Med. Sci. Monit. **8:**RA119–RA127.
25. **Masayama, A., H. Fukuoka, S. Kato, T. Yoshimura, M. Moriyama, and R. Moriyama.** 2006. Subcellular localization of a germiantion-specific cortex-lytic enzyme, SleB, of bacilli during sporulation. Genes Genet. Syst. **81:**163–169.
26. **Meador-Parton, J., and D. L. Popham.** 2000. Structural analysis of *Bacillus subtilis* spore peptidoglycan during sporulation. J. Bacteriol. **182:**4491–4499.
27. **Miller, J. H.** 1972. Experiments in molecular genetics. Cold Spring Harbor Laboratories, Cold Spring Harbor, NY.
28. **Miyata, S., R. Moriyama, N. Miyahara, and S. Makino.** 1995. A gene (*sleC*) encoding a spore-cortex-lytic enzyme from *Clostridium perfringens* S40 spores; cloning, sequence analysis and molecular characterization. Microbiology **141:**2643–2650.
29. **Moir, A.** 2006. How do spores germinate? J. Appl. Microbiol. **101:**526–530.
30. **Moir, A., B. M. Corfe, and J. Behravan.** 2002. Spore germination. Cell. Mol. Life Sci. **59:**403–409.
31. **Morgulis, A., G. Coulouris, Y. Raytselis, T. L. Madden, R. Agarwala, and A. A. Schaffer.** 2008. Database indexing for production MegaBLAST searches. Bioinformatics **24:**1757–1764.
32. **Moriyama, R., H. Fukuoka, S. Miyata, S. Kudoh, A. Hattori, S. Kozuka, Y. Yasuda, K. Tochikubo, and S. Makino.** 1999. Expression of a germination-specific amidase, SleB, of bacilli in the forespore compartment of sporulating cells and its localization on the exterior side of the cortex in dormant spores. J. Bacteriol. **181:**2373–2378.
33. **Moriyama, R., A. Hattori, S. Miyata, S. Kudoh, and S. Makino.** 1996. A gene (*sleB*) encoding a spore cortex-lytic enzyme from *Bacillus subtilis* and response of the enzyme to L-alanine-mediated germination. J. Bacteriol. **178:**6059–6063.
34. **Nicholson, W. L., and P. Setlow.** 1990. Sporulation, germination, and outgrowth, p. 391–450. *In* C. R. Harwood and S. M. Cutting (ed.), Molecular biological methods for *Bacillus*. John Wiley & Sons, Ltd., Chichester, England.
35. **Orsburn, B., S. B. Melville, and D. L. Popham.** 2008. Factors contributing to heat resistance of *Clostridium perfringens* endospores. Appl. Environ. Microbiol. **74:**3328–3335.
36. **Paidhungat, M., K. Ragkousi, and P. Setlow.** 2001. Genetic requirements for induction of germination of spores of *Bacillus subtilis* by Ca^{2+}-dipicolinate. J. Bacteriol. **183:**4886–4893.
37. **Popham, D. L., J. Helin, C. E. Costello, and P. Setlow.** 1996. Muramic lactam in peptidoglycan of *Bacillus subtilis* spores is required for spore outgrowth but not for spore dehydration or heat resistance. Proc. Natl. Acad. Sci. USA **93:**15405–15410.
38. **Quinn, C. P., and B. N. Dancer.** 1990. Transformation of vegetative cells of *Bacillus anthracis* with plasmid DNA. J. Gen. Microbiol. **136:**1211–1215.
39. **Ragkousi, K., P. Eichenberger, C. van Ooij, and P. Setlow.** 2003. Identification of a new gene essential for germination of *Bacillus subtilis* spores with Ca^{2+}-dipicolinate. J. Bacteriol. **185:**2315–2329.
40. **Schleifer, K. H., and O. Kandler.** 1972. Peptidoglycan types of bacterial cell walls and their taxonomic implications. Bacteriol. Rev. **36:**407–477.
41. **Setlow, B., E. Melly, and P. Setlow.** 2001. Properties of spores of *Bacillus subtilis* blocked at an intermediate stage in spore germination. J. Bacteriol. **183:**4894–4899.
42. **Setlow, P.** 2006. Spores of *Bacillus subtilis*: their resistance to and killing by radiation, heat and chemicals. J. Appl. Microbiol. **101:**514–525.
43. **Warth, A. D., and J. L. Strominger.** 1969. Structure of the peptidoglycan of bacterial spores: occurrence of the lactam of muramic acid. Proc. Natl. Acad. Sci. USA **64:**528–535.
44. **Zhang, Z., S. Schwartz, L. Wagner, and W. Miller.** 2000. A greedy algorithm for aligning DNA sequences. J. Comput. Biol. **7:**203–214.